Trigonometric pulse envelopes for laser induced quantum dynamics

I. Barth[1] **and C. Lasser**[2]

[1] Institut für Chemie und Biochemie, Freie Universität Berlin, Takustr. 3, 14195 Berlin, Germany

[2] Fachbereich Mathematik, Freie Universität Berlin, Arnimallee 6, 14195 Berlin, Germany

E-mail: barth@chemie.fu-berlin.de, lasser@math.fu-berlin.de

Abstract. We relate powers of trigonometric functions to Gaussians by proving, that properly truncated $\cos^n$ functions converge to a Gaussian as n tends to infinity. For an application, we analyse the laser induced population transfer $|X\,^1\Sigma^+\rangle \to |A\,^1\Pi_x\rangle$ in a two-level model system of aluminium monochloride (AlCl) with fixed nuclei. We apply linearly x-polarized ultraviolet laser pulses with trigonometric envelope function, whose square has full width at half maximum of 2.5 fs and 5.0 fs. Studying population dynamics and optimized laser parameters, we find that the optimal field amplitude for trigonometric pulses with $n = 20$ and $n = 1000$ have a relative difference of one percent, which is below experimental resolution.

PACS numbers: 33.80.-b, 02.30.Nw

Submitted to: *J. Phys. B: At. Mol. Opt. Phys.*

1. Introduction

Experiments often use Gaussian laser pulses. Hence, for quantum dynamics simulations, various pulse envelope functions of Gaussian form are employed: $\sin^2$ pulses [1–12] or equivalent $\cos^2$ pulses [13–15], $\sin^4$ pulses [16], $\sin^{2n}$ pulses [17], $\cos^{20}$ pulses [18–22], sech pulses [17,23], triangular pulses [3], trapezoidal pulses [24] or time-cutted Gaussian pulses [3, 24–29]. This variety reflects different rankings of somehow incompatible modelling requirements as finite pulse duration, higher order differentiability, or an manageable analytical expression.

It is our aim and main contribution here to mathematically relate trigonometric pulse envelopes with Gaussian functions. We prove, that in the limit $n \to \infty$ suitably truncated $\cos^n$ functions converge to a Gaussian, whose square has the same full width at half maximum. The trigonometric pulse envelopes have a finite support in the time domain and gain higher order differentiability when the exponent value n increases.

As an exemplary application, we choose a laser induced molecular transition. We consider a simple two-level model for the linear molecule aluminium monochloride (AlCl) with pre-orientation in z-direction [22, 30, 31] and study the laser induced optimal total population transfer from the electronic ground state $|X\,{}^1\Sigma^+\rangle$ to the first electronic excited state $|A\,{}^1\Pi_x\rangle$. We use linearly x-polarized ultraviolet laser pulses with trigonometric envelope, whose square has full width at half maximum of 2.5 fs [21] and 5.0 fs. On the short time scale considered, we assume that the nuclei stay fixed and that other electronic states can be neglected to obtain a two-level ordinary differential system. For this system, we numerically explore the influence of the $\cos^n$ envelope on the population dynamics and on optimized laser parameters for achieving maximal population transfer. We also mention, that recent work on AlCl [21] and BeO [22] has addressed strong electronic ring currents of the first electronic degenerate excited states $|A\,{}^1\Pi_\pm\rangle$ and associated strong induced magnetic fields generated by circularly polarized laser pulses with trigonometric envelope.

The article is organized as follows. Section 2 defines the trigonometric envelopes, discusses their limiting behavior and their spectral width. Then, Section 3 introduces the model for the electronic excitation of AlCl. Section 4 collects the numerical results, and Section 5 offers some concluding remarks. The mathematical proofs are given in the Appendices A, B, and C.

2. Trigonometric pulse envelopes

2.1. Laser pulse

For the modeling of a linearly x-polarized laser pulse one starts by defining a time-dependent vector-potential $\mathbf{A}(t) = A_x(t)\mathbf{e}_x$ that has a non-vanishing component only in x-direction. Denoting the laser amplitude by $\mathcal{E}_0$, the carrier frequency by ω, and the

carrier envelope phase by $\eta \in [0, 2\pi)$, we set

$$A_x(t) = -\frac{\mathcal{E}_0}{\omega} s_n(t) \sin(\omega t + \eta).$$

For the slowly varying envelope function $s_n(t) : (-\infty, \infty) \to [0, 1]$ one has to make a choice. Here, we investigate trigonometric pulse envelopes

$$s_n(t) = \begin{cases} \cos^n\left(\frac{\pi t}{T_n}\right) & \text{for} \quad |t| \leq \frac{T_n}{2}, \\ 0 & \text{for} \quad |t| > \frac{T_n}{2} \end{cases} \tag{1}$$

with exponent $n > 0$. We define the n-dependent total pulse duration $T_n > 0$,

$$T_n = \frac{\pi \tau}{f_n}, \qquad f_n = 2 \arccos\left(2^{-\frac{1}{2n}}\right),$$

such that $\tau > 0$ is the full width at half maximum of $s_n^2(t)$, that is, $s_n^2(\tau/2) = \frac{1}{2}$. We note, that $s_n(t)$ for $n > 1$ is continuously differentiable. As in [13, 18–23, 28, 29], the time-dependent electric field $\mathbf{E}(t) = \mathcal{E}_x(t)\mathbf{e}_x$ is derived from the vector potential $\mathbf{A}(t)$ by setting

$$\mathcal{E}_x(t) = -\frac{\mathrm{d}}{\mathrm{d}t} A_x(t) = \mathcal{E}_0 s_n(t) \cos(\omega t + \eta) + \frac{\mathcal{E}_0}{\omega} \left[\frac{\mathrm{d}}{\mathrm{d}t} s_n(t)\right] \sin(\omega t + \eta). \tag{2}$$

By construction, the zero frequency or direct current component of the electric field vanishes,

$$\int_{-\infty}^{\infty} \mathbf{E}(t) \mathrm{d}t = \mathbf{0},$$

which is in accordance with the far-field approximation of Maxwell's equations [29, 32]. Moreover, the electric field $\mathbf{E}(t)$ for $n > 2$ is continuously differentiable.

2.2. Limiting behavior

We first discuss the behavior of the trigonometric pulse envelopes $s_n(t)$ when passing to the limit $n \to \infty$, which links it to the conventional Gaussian envelope functions. Then, we consider the regime of large numbers of laser cycles and interpret τ as the effective pulse duration.

A Gaussian function $s(t) : (-\infty, \infty) \to [0, 1]$, such that τ is the full width at half maximum of its square, has the form $s(t) = \exp(-2\ln(2)t^2/\tau^2)$. In the Appendix A, we prove the convergence of

$$\mathrm{e}^{-t^2} = \lim_{n\to\infty} \cos^n\left(\sqrt{\frac{2}{n}}\, t\right), \qquad s(t) = \lim_{n\to\infty} s_n(t),$$

which both are uniform in every bounded time interval $|t| \leq R$ with $R > 0$. The plots in figures 1 and 2 illustrate, that the convergence is rather fast. For $n = 20$, the maximal deviation between the trigonometric envelope and the Gaussian is already 0.0077.

The full width at half maximum τ of the squared envelope can be considered as the effective pulse duration. Let ε_0 and c denote the permittivity of vacuum and speed of light, respectively. Then, the envelope of the time-dependent intensity $I(t) = c\varepsilon_0 \mathcal{E}_x^2(t)$

has approximately the same full width at half maximum as $s_n^2(t)$, if the number of laser cycles is large. Indeed, for large carrier frequencies ω, the electric field and the intensity satisfy

$$\mathcal{E}_x(t) \approx \mathcal{E}_0 s_n(t)\cos(\omega t+\eta), \qquad I(t) \approx c\varepsilon_0 \mathcal{E}_0^2 s_n^2(t)\cos^2(\omega t+\eta).$$

Thus, the full width at half maximum of $s_n^2(t)$ and of the envelope of $I(t)$ approximately coincide.

2.3. Spectral width

We denote the Fourier transform of the trigonometric envelope by

$$\hat{s}_n(k) = \frac{1}{\sqrt{2\pi}} \int_{-\infty}^{\infty} s_n(t) \mathrm{e}^{-\mathrm{i}kt}\,\mathrm{d}t.$$

Since $\lim_{n\to\infty} s_n(t) = s(t)$ holds uniformly on bounded time intervals, the Fourier transform converges pointwise to a Gaussian. That is,

$$\lim_{n\to\infty} \hat{s}_n(k) = \hat{s}(k) = \frac{1}{\sqrt{2\pi}} \int_{-\infty}^{\infty} s(t)\mathrm{e}^{-\mathrm{i}kt}\,\mathrm{d}t = \frac{\tau}{2\sqrt{\ln(2)}}\,\mathrm{e}^{-k^2\tau^2/[8\ln(2)]}$$

for all $k \in (-\infty,\infty)$. The Fourier transform can be expressed in closed form in terms of the Gamma function. We have for all real numbers $n > 0$ and $k \in (-\infty,\infty)$

$$\hat{s}_n(k) = \frac{2^{-n-1/2}\sqrt{\pi}\,\Gamma(n+1)\,\tau}{f_n \Gamma\left(1+\frac{n}{2}-\frac{k\tau}{2f_n}\right)\Gamma\left(1+\frac{n}{2}+\frac{k\tau}{2f_n}\right)}. \tag{3}$$

Such Gamma function formulae are discussed for example in Titchmarsh's monograph on Fourier integrals [33], see also Appendix B. For $n \in \mathbb{N}$ the Fourier transform can be rewritten with trigonometric functions as

$$\hat{s}_n(k) = \begin{cases} -\dfrac{2^{-n-3/2}\,n!\,\tau^2 k \sin\left(\frac{\pi k\tau}{2f_n}\right)}{\sqrt{\pi} f_n^2 \prod_{j=0}^{\frac{n}{2}}\left[j^2-\left(\frac{k\tau}{2f_n}\right)^2\right]}, & n \text{ even}, \\[2ex] \dfrac{2^{-n-1/2}\,n!\,\tau \cos\left(\frac{\pi k\tau}{2f_n}\right)}{\sqrt{\pi} f_n \prod_{j=0}^{\frac{n}{2}-\frac{1}{2}}\left[\left(j+\frac{1}{2}\right)^2-\left(\frac{k\tau}{2f_n}\right)^2\right]}, & n \text{ odd}, \end{cases}$$

see Appendix C. The maximal deviation between $\hat{s}_n(k)$ and $\hat{s}(k)$ is found at $k = 0$, and the corresponding relative deviation for $n = 20$ is $|\hat{s}_{20}(0) - \hat{s}(0)|/|\hat{s}(0)| = 0.0096$, illustrating the fast convergence of the Fourier transform of the trigonometric envelope.

The full width at half maximum of $\hat{s}^2(k)$ is easily evaluated as $\kappa = 4\ln 2/\tau$, while for determining the full width at half maximum κ_n of $\hat{s}_n^2(k)$ one has to numerically solve a nonlinear equation. Table 1 lists the numerical coefficients $c_n = \kappa_n\tau$ of trigonometric envelopes as well as $c = \kappa\tau$ of the Gaussian envelope. Note that c_n and c are independent of the effective pulse duration τ because κ_n and κ are inversely proportional to τ. We obtain the relative difference $|c_{20} - c|/|c| = 0.0193$, indicating that the spectral width $\Gamma_n = \kappa_n\hbar = c_n\hbar/\tau$ converges to $\Gamma = \kappa\hbar = c\hbar/\tau$ slightly slower than the maximal deviation of the Fourier transforms.

3. Off-diagonal two-level systems

We first discuss our modelling assumptions for electronic excitation by linearly x-polarized laser pulses. Then, we apply the model to the diatomic molecule AlCl with the molecular symmetry $C_{\infty,v}$ pre-oriented in z-direction, see also [22, 30, 31].

3.1. Derivation of the model

We assume, that the molecule's electronic Hamilton operator has two eigenstates with equal equilibrium configuration of the molecule. Orbital symmetries and gap sizes in the electronic spectrum allow linearly x-polarized laser excitation only between these two states. Moreover, the vibrational period of the molecule is considerably longer than the effective pulse duration τ, and one assumes the nuclei fixed at the equilibrium configuration. We denote the electronic Hamiltonian for fixed nuclei by H_{el}. The two eigenstates under consideration solve the electronic eigenvalue problem $H_{\mathrm{el}}|\Psi_1\rangle = E_1|\Psi_1\rangle$ and $H_{\mathrm{el}}|\Psi_2\rangle = E_2|\Psi_2\rangle$. If x_i and X_j are the x-component of the position of the i-th electron and j-th nucleus, N and $\hat{N}$ the total number of electrons and nuclei of the molecule, $-e$ and $Z_j e$ the electronic charge and charge of the j-th nucleus, respectively, then the x-component of the dipole operator writes as

$$M_x = -e\sum_{i=1}^{N} x_i + e\sum_{j=1}^{\hat{N}} Z_j X_j.$$

We additionally assume that the transition dipole matrix is real-symmetric and off-diagonal,

$$\begin{pmatrix} \langle\Psi_1|M_x|\Psi_1\rangle & \langle\Psi_1|M_x|\Psi_2\rangle \\ \langle\Psi_2|M_x|\Psi_1\rangle & \langle\Psi_2|M_x|\Psi_2\rangle \end{pmatrix} =: \begin{pmatrix} 0 & M \\ M & 0 \end{pmatrix}.$$

Then, the electric dipole approximation of the laser driven electron dynamics starting in the electronic eigenstate $|\Psi_1\rangle$ is given by the time-dependent electronic Schrödinger equation

$$\mathrm{i}\hbar\frac{\mathrm{d}}{\mathrm{d}t}|\Psi(t)\rangle = [H_{\mathrm{el}} - M_x\mathcal{E}_x(t)]\,|\Psi(t)\rangle, \qquad |\Psi(-T_n/2)\rangle = |\Psi_1\rangle \tag{4}$$

where the electric field $\mathcal{E}_x(t)$ is defined in (2) using the trigonometric envelope $s_n(t)$ given in (1). We insert the ansatz $|\Psi(t)\rangle = C_1(t)|\Psi_1\rangle + C_2(t)|\Psi_2\rangle$ into the time-dependent Schrödinger equation (4). Due to the assumption that the electronic transition is only possible between two states under consideration, we obtain an ordinary differential equation for the time-dependent coefficient vector $C(t) = (C_1(t), C_2(t))^T$,

$$\begin{aligned} \mathrm{i}\hbar\frac{\mathrm{d}}{\mathrm{d}t}C(t) &= \left[\begin{pmatrix} E_1 & 0 \\ 0 & E_2 \end{pmatrix} - M\mathcal{E}_x(t)\begin{pmatrix} 0 & 1 \\ 1 & 0 \end{pmatrix}\right] C(t), \\ C(-T_n/2) &= \begin{pmatrix} 1 \\ 0 \end{pmatrix}. \end{aligned} \tag{5}$$

3.2. Application to a model system of AlCl

In the following, we use quantum chemistry results for AlCl by Langhoff et al. [34]. The ground state $|\Psi_1\rangle = |X\,{}^1\Sigma^+\rangle$ and the first excited singlet state $|\Psi_2\rangle = |A\,{}^1\Pi_x\rangle$ satisfy our assumptions. Indeed, the excitation energy from $|X\,{}^1\Sigma^+\rangle$ to $|A\,{}^1\Pi_x\rangle$ is $\hbar\hat{\omega} = E_2 - E_1 =$ 4.79 eV. The excitation energy for the next excited ${}^1\Pi_x$ state is considerably higher, namely 8.56 eV, see [21]. Moreover, starting from the ground state $|X\,{}^1\Sigma^+\rangle$ and using linearly x-polarized laser pulses, the populations of excited degenerates states ${}^1\Pi_y$ are always zero, and direct dipole transitions from the ground state $|X\,{}^1\Sigma^+\rangle$ to other excited states of type $\Sigma^+, \Delta, \Phi, \ldots$ are not allowed. The equilibrium bond length of the both states $|X\,{}^1\Sigma^+\rangle$ and $|A\,{}^1\Pi_x\rangle$ is almost equal ($R_X = 4.055\,a_0$ and $R_A = 4.067\,a_0$).

The heavy molecule AlCl has the experimental vibration frequency of $\omega_e = 481\,hc\,\mathrm{cm}^{-1}$ [35] with the corresponding period of $T_{vib} = 69\,\mathrm{fs}$. We choose the effective pulse duration $\tau = 2.5\,\mathrm{fs}$ or $\tau = 5.0\,\mathrm{fs}$. Figure 2 illustrates, that for $n = 20$ the total pulse duration is $T_n = 21\,\mathrm{fs}$ or $T_n = 42\,\mathrm{fs}$, respectively. Hence, the nuclei are assumed to stay fixed during the pulse. By the symmetry of ${}^1\Sigma^+$ and ${}^1\Pi_x$ states, the transition dipole matrix is real-symmetric and off-diagonal with $M = 1.33\,ea_0$. Therefore, the electron dynamics of the z-oriented AlCl molecule driven by a linearly x-polarized laser pulse may be modelled by an off-diagonal two-level system of the form (5).

4. Numerical results

We concentrate on the regime of large numbers of laser cycles, where total population transfer from $|X\,{}^1\Sigma^+\rangle$ to $|A\,{}^1\Pi_x\rangle$ is only achieved for a laser frequency ω close to the excitation frequency $\hat{\omega}$ and for a laser amplitude $\mathcal{E}_0$ close to the reference amplitude $\hat{\mathcal{E}}_0 = 2\pi\hbar/(MT_2)$ of the π-pulse with $n = 2$, that is, $\hat{\mathcal{E}}_0 = 4.28\,\mathrm{GVm}^{-1}$ and $\hat{\mathcal{E}}_0 = 8.56\,\mathrm{GVm}^{-1}$ for $\tau = 2.5\,\mathrm{fs}$ and $\tau = 5.0\,\mathrm{fs}$, respectively, see [36]. We set $\eta = \pi/2$ and optimize the two remaining parameters $\mathcal{E}_0$ and ω of the electric field for maximal transfer from $|X\,{}^1\Sigma^+\rangle$ to $|A\,{}^1\Pi_x\rangle$ at the end of the pulse at time $t = T_n/2$. We therefore numerically solve the differential system (5) for various exponent values $n = 2, 5, 20, 1000$ and effective pulse durations $\tau = 2.5\,\mathrm{fs}$ and $\tau = 5.0\,\mathrm{fs}$. We use a fourth order Runge-Kutta method, which in all calculations numerically converges for a step size of 1 as.

The resulting optimal parameters are given in table 2. For growing exponent values n, there is a monotonous increase of the optimal laser frequency ω towards the excitation frequency $\hat{\omega} = 4.79\,\mathrm{eV}/\hbar$. The relative difference between the values for $n = 20$ and $n = 1000$ is less than one permille. Moreover, the frequencies for the longer pulse with $\tau = 5.0\,\mathrm{fs}$ are closer to the excitation frequency $\hat{\omega}$ than those for the shorter pulse with $\tau = 2.5\,\mathrm{fs}$, since the error depends on the size of the second term of the electric field in (2), which is proportional to the inverse of τ. The optimal laser amplitude $\mathcal{E}_0$ monotonously decreases with growing n, because the total pulse duration T_n increases with growing n. The relative difference between the values for $n = 20$ and $n = 1000$ is one percent, which is below experimental resolution. As for the reference π pulses, the

amplitudes for the $\tau = 2.5\,\mathrm{fs}$ pulse are roughly twice the ones for the $\tau = 5.0\,\mathrm{fs}$ pulse.

Figure 3 illustrates the time evolution of the populations $P_A(t) = |C_2(t)|^2$ of the first excited state $|A\,{}^1\Pi_x\rangle$ for four different classes of pulse envelopes. Qualitatively, all plots show the same monotonous step-like increase up to a population of 98 to almost 100 percent. For the longer pulses with $\tau = 5.0\,\mathrm{fs}$ the number of steps is approximately twice the number for the shorter pulses with $\tau = 2.5\,\mathrm{fs}$. In figure 3(a), the dynamics are plotted for laser parameters, which are optimal for the pulse with $n = 1000$. The four curves get closer to each other for growing values of n. The maximal deviation between the $n = 2$ and $n = 1000$ population is around five percent. Figure 3(b) shows the corresponding results, when the laser parameters are chosen in an optimal way for each exponent n independently. In this case, the curves almost match. Figure 4 plots the final populations $P_A(T_n/2)$ of the first excited state versus $\log_{10} n$. The laser parameters are the optimal ones for $n = 1000$. The results for $\tau = 2.5\,\mathrm{fs}$ and $\tau = 5.0\,\mathrm{fs}$ agree within graphical resolution. For $n = 20$, for example, the final population is 99.98 percent.

5. Conclusions

We have related powers of trigonometric pulse envelopes to Gaussian functions in the limit of the exponent n tending to infinity. The trigonometric envelopes $s_n(t)$ combine the advantages of modelling finite pulse duration with high order differentiability. We note that the nonnegative function $K_n(t) = s_n(t)/(\sqrt{2\pi}\,\hat{s}_n(0))$ can be interpreted as a normalized probability density function with expectation value zero. Therefore, the trigonometric envelopes could also serve in nonparametric density estimation, where various choices of kernels with finite support are discussed, see [37]. The numerical experiments for the laser excitation of AlCl show a regular and convergent behavior with respect to the exponent n. In the regime of large numbers of laser cycles, optimized laser parameters for $n = 20$ and $n = 1000$ have a relative difference of less than one percent, which is below experimental resolution. Future work should explore the complementary regime of few-cycle laser pulses.

Acknowledgments

We would like to thank to J. Manz (FU Berlin) and M. Kitzler (TU Wien) for stimulating discussions. Financial support by the Deutsche Forschungsgemeinschaft (Sfb 450, TPC1 and TPC5) is also gratefully acknowledged.

Appendix A. Convergence proofs

Proof 1

We prove the convergence of

$$\mathrm{e}^{-t^2} = \lim_{n\to\infty} \cos^n\left(\sqrt{\frac{2}{n}}\,t\right), \tag{A.1}$$

which is uniform in $|t| \leq R$ for all $R > 0$. By the infinite product formula for the cosine

$$\cos(t) \;=\; \prod_{j=1}^{\infty} \left[1 - \frac{4t^2}{\pi^2\,(2j-1)^2}\right],$$

which converges uniformly in $|t| \leq R$, see for example [38], we obtain

$$\lim_{n\to\infty} \cos^n\left(\sqrt{\frac{2}{n}}\,t\right) = \lim_{n\to\infty} \prod_{j=1}^{\infty} \left[1 - \frac{8t^2}{n\pi^2\,(2j-1)^2}\right]^n.$$

A product $\prod_{j=1}^{\infty}[1 + a_j(x)]$ converges uniformly in x, if and only if the series $\sum_{j=1}^{\infty} \ln[1 + a_j(x)]$ converges uniformly in x [39]. Hence, the bound

$$\left| n \ln\left[1 - \frac{8t^2}{n\pi^2\,(2j-1)^2}\right]\right| \leq \frac{16t^2}{\pi^2(2j-1)^2}$$

for n sufficiently large implies uniform convergence of the infinite product and consequently

$$\lim_{n\to\infty} \cos^n\left(\sqrt{\frac{2}{n}}\,t\right) = \prod_{j=1}^{\infty} \lim_{n\to\infty} \left[1 - \frac{8t^2}{n\pi^2\,(2j-1)^2}\right]^n.$$

Since $\lim_{n\to\infty}(1 + x/n)^n = \mathrm{e}^x$ uniformly in $|x| \leq R$ and $\sum_{j=1}^{\infty} 1/(2j-1)^2 = 3/4\sum_{j=1}^{\infty} 1/j^2 = \pi^2/8$, we get

$$\begin{aligned}\lim_{n\to\infty} \cos^n\left(\sqrt{\frac{2}{n}}\,t\right) &= \prod_{j=1}^{\infty} \exp\left[-\frac{8t^2}{\pi^2\,(2j-1)^2}\right] \\ &= \exp\left[-\frac{8t^2}{\pi^2} \sum_{j=1}^{\infty} \frac{1}{(2j-1)^2}\right] = \mathrm{e}^{-t^2}\end{aligned}$$

uniformly in $|t| \leq R$. $\diamondsuit$

We note that uniform convergence of the limit (A.1) is needed for proving the convergence of the trigonometric pulse envelopes to a Gaussian function. However, there is also a more elementary argument for proving pointwise convergence using l'Hospital's rule, see [40].

Proof 2

It remains to prove the uniform convergence of $s(t) = \lim_{n\to\infty} s_n(t)$ for $|t| \leq R$. Since $f_n = 2\arccos\left(2^{-1/(2n)}\right) \to 0$ and $T_n = \pi\tau/f_n \to \infty$ as $n \to \infty$, one has $R \leq T_n/2$ for n sufficiently large, and we only need to verify that

$$\mathrm{e}^{-2\ln(2)t^2/\tau^2} = \lim_{n\to\infty} \cos^n\left(\frac{t}{\tau}\,f_n\right)$$

uniformly in $|t| \leq R$. By l'Hospital's rule, $\lim_{n\to\infty} n\left(1 - 2^{-1/n}\right) = \ln(2)$ and

$$\begin{aligned}\lim_{n\to\infty} \sqrt{n} f_n &= \lim_{n\to\infty} \frac{-\left(1 - 2^{-1/n}\right)^{-1/2}\, 2^{-\frac{1}{2n}} n^{-2} \ln(2)}{-\frac{1}{2} n^{-3/2}} \\ &= 2\ln(2) \lim_{n\to\infty} \frac{2^{-\frac{1}{2n}}}{\sqrt{n\,(1 - 2^{-1/n})}} = 2\sqrt{\ln(2)}.\end{aligned}$$

Then, we have uniformly in $|t| \leq R$

$$\left|\cos^n\left(\frac{t}{\tau}\, f_n\right) - \mathrm{e}^{-2\ln(2)t^2/\tau^2}\right| \leq \left|\cos^n\left(\frac{t}{\tau}\, f_n\right) - \mathrm{e}^{-\left(\sqrt{\frac{n}{2}}\frac{t}{\tau} f_n\right)^2}\right| + \left|\mathrm{e}^{-\left(\sqrt{\frac{n}{2}}\frac{t}{\tau} f_n\right)^2} - \mathrm{e}^{-2\ln(2)t^2/\tau^2}\right| \overset{n\to\infty}{\longrightarrow} 0,$$

where the first and second difference tend to zero because of the uniform convergence in formula (A.1) and continuity of the Gaussian function $x \mapsto \exp(-x^2)$, respectively. $\diamondsuit$

Appendix B. Fourier transform

One observes

$$\int_{-\frac{\pi\tau}{2f_n}}^{\frac{\pi\tau}{2f_n}} \cos^n\left(\tfrac{f_n t}{\tau}\right) \mathrm{e}^{-\mathrm{i}kt}\mathrm{d}t = \frac{\tau}{f_n}\int_{-\frac{\pi}{2}}^{\frac{\pi}{2}} \cos^n(\theta)\mathrm{e}^{-\mathrm{i}\frac{k\tau}{f_n}\theta}\mathrm{d}\theta.$$

Using $k' = -k\tau/f_n$, the formula for the Fourier transform (3) is therefore equivalent to

$$\int_{-\frac{\pi}{2}}^{\frac{\pi}{2}} \cos^n(\theta)\mathrm{e}^{\mathrm{i}k'\theta}\mathrm{d}\theta = \frac{2^{-n}\pi\Gamma(n+1)}{\Gamma\left(1+\frac{n}{2}+\frac{k'}{2}\right)\Gamma\left(1+\frac{n}{2}-\frac{k'}{2}\right)} \tag{B.1}$$

for all real numbers $n > 0$ and $k' \in (-\infty, \infty)$. This Gamma function formula, however, is well-known [41]. In [33], Titchmarsh indicates that the formula may be obtained by calculating

$$\int \left(w + w^{-1}\right)^n w^{k'-1}\mathrm{d}w,$$

along the contour, which is formed by joining $-\mathrm{i}$ and i by the imaginary axis and by the right half of the unit circle.

Indeed, let Γ be the right half of the unit circle in counter-clockwise orientation, Γ_δ the right half of the circle with radius $0 < \delta < 1$ centered at the origin in counter-clockwise orientation, Γ_+ and Γ_- the parts of the imaginary axis between $\mathrm{i}\delta$ and i respectively $-\mathrm{i}\delta$ and $-\mathrm{i}$. We take $\log w = \log\rho + \mathrm{i}\theta$ if $w = \rho\mathrm{e}^{\mathrm{i}\theta}$ with $\theta \in (-\pi, \pi)$ and obtain

$$\begin{aligned}\int_\Gamma \left(w + w^{-1}\right)^n w^{k'-1}\mathrm{d}w &= \mathrm{i}\int_{-\frac{\pi}{2}}^{\frac{\pi}{2}} \left(\mathrm{e}^{\mathrm{i}\theta} + \mathrm{e}^{-\mathrm{i}\theta}\right)^n \mathrm{e}^{\mathrm{i}k'\theta}\mathrm{d}\theta \\ &= \mathrm{i}2^n\int_{-\frac{\pi}{2}}^{\frac{\pi}{2}} \cos^n(\theta)\mathrm{e}^{\mathrm{i}k'\theta}\mathrm{d}\theta.\end{aligned}$$

Let $k' \geq n > 0$. There exists $C > 0$ such that for all $w \in \Gamma_\delta$.

$$\left|\left(w + w^{-1}\right)^n w^{k'-1}\right| = \left|\left(w^2+1\right)^n w^{k'-n-1}\right| \leq C\delta^{k'-n-1}.$$

Therefore,

$$\int_{\Gamma_\delta} \left(w + w^{-1}\right)^n w^{k'-1}\mathrm{d}w \overset{\delta\to 0}{\longrightarrow} 0.$$

Moreover,

$$\begin{aligned}\int_{\Gamma_\pm}\left(w+w^{-1}\right)^n w^{k'-1}\mathrm{d}w &= \int_{\Gamma_\pm}\left(w^2+1\right)^n w^{k'-n-1}\mathrm{d}w\\ &= \int_\delta^1\left(-\rho^2+1\right)^n\rho^{k'-n-1}\mathrm{e}^{\pm\mathrm{i}(k'-n-1)\pi/2}\mathrm{e}^{\pm\mathrm{i}\pi/2}\mathrm{d}\rho\\ &\xrightarrow{\delta\to 0}\mathrm{e}^{\pm\mathrm{i}(k'-n)\pi/2}\int_0^1\left(-\rho^2+1\right)^n\rho^{k'-n-1}\mathrm{d}\rho.\end{aligned}$$

The latter integral can be rewritten using the Euler Beta function

$$B(q,p)=\int_0^1 x^{p-1}(1-x)^{q-1}\mathrm{d}x=\frac{\Gamma(q)\Gamma(p)}{\Gamma(q+p)}$$

for $p,q>0$, see [39]. Indeed,

$$\begin{aligned}\int_0^1\left(1-\rho^2\right)^n\rho^{k'-n-1}\mathrm{d}\rho &= \frac{1}{2}\int_0^1(1-x)^n x^{k'/2-n/2-1}\mathrm{d}x\\ &= \frac{1}{2}B\left(\tfrac{k'}{2}-\tfrac{n}{2},n+1\right),\end{aligned}$$

which is valid for $n>-1$. Therefore, the equality

$$\begin{aligned}0=&\int_\Gamma\left(w+w^{-1}\right)^n w^{k'-1}\mathrm{d}w-\int_{\Gamma_+}\left(w+w^{-1}\right)^n w^{k'-1}\mathrm{d}w\\ &-\int_{\Gamma_\delta}\left(w+w^{-1}\right)^n w^{k'-1}\mathrm{d}w+\int_{\Gamma_-}\left(w+w^{-1}\right)^n w^{k'-1}\mathrm{d}w\end{aligned}$$

implies for the limit $\delta\to 0$

$$\begin{aligned}\int_\Gamma\left(w+w^{-1}\right)^n w^{k'-1}\mathrm{d}w &= \frac{1}{2}\left(\mathrm{e}^{\mathrm{i}(k'-n)\pi/2}-\mathrm{e}^{-\mathrm{i}(k'-n)\pi/2}\right)B\left(\frac{k'}{2}-\frac{n}{2},n+1\right)\\ &= \mathrm{i}\sin\left[\pi\left(\frac{k'}{2}-\frac{n}{2}\right)\right]\frac{\Gamma(\frac{k'}{2}-\frac{n}{2})\Gamma(n+1)}{\Gamma\left(1+\frac{n}{2}+\frac{k'}{2}\right)}.\end{aligned}$$

Since $\Gamma(z)\Gamma(1-z)=\pi/\sin(\pi z)$, see [39], one has

$$\Gamma\left(\frac{k'}{2}-\frac{n}{2}\right)=\frac{\pi}{\sin\left[\pi\left(\frac{k'}{2}-\frac{n}{2}\right)\right]\Gamma\left(1+\frac{n}{2}-\frac{k'}{2}\right)},$$

and consequently

$$\begin{aligned}\int_{-\frac{\pi}{2}}^{\frac{\pi}{2}}\cos^n(\theta)\mathrm{e}^{\mathrm{i}k'\theta}\mathrm{d}\theta &= -\mathrm{i}2^{-n}\int_\Gamma\left(w+w^{-1}\right)^n w^{k'-1}\mathrm{d}w\\ &= \frac{2^{-n}\pi\Gamma(n+1)}{\Gamma\left(1+\frac{n}{2}+\frac{k'}{2}\right)\Gamma\left(1+\frac{n}{2}-\frac{k'}{2}\right)}.\end{aligned}$$

For fixed n, both expressions on the left and the right handside of (B.1) define functions, which are holomorphic for k' in the entire complex plane. Therefore, the restriction $k'\geq n$ can be removed, and the claimed identity holds for all real $n>0$ and $k'\in(-\infty,\infty)$.

Appendix C. Product of Gamma functions

We rewrite the product of Gamma functions $\Gamma\left(1+n/2-x\right)\Gamma\left(1+n/2+x\right)$ for all $n \in \mathbb{N}$ in terms of trigonometric functions as follows. Using the crucial properties of the Gamma function

$$\Gamma(1+x) = x\Gamma(x), \quad \Gamma(1-x)\Gamma(x) = \frac{\pi}{\sin(\pi x)},$$

see [39], we obtain for even n

$$\begin{aligned}\Gamma\left(1+\frac{n}{2}-x\right)\Gamma\left(1+\frac{n}{2}+x\right) &= -\frac{1}{x}\,\Gamma(1-x)\Gamma(x)\prod_{j=0}^{\frac{n}{2}}(j-x)(j+x)\\ &= -\frac{\pi}{x\sin(\pi x)}\prod_{j=0}^{\frac{n}{2}}\left(j^2-x^2\right)\end{aligned}$$

and for odd n

$$\begin{aligned}&\Gamma\left(1+\frac{n}{2}-x\right)\Gamma\left(1+\frac{n}{2}+x\right)\\ &\quad= \Gamma\left[1-\left(\frac{1}{2}+x\right)\right]\Gamma\left(\frac{1}{2}+x\right)\prod_{j=0}^{\frac{n}{2}-\frac{1}{2}}\left(j+\frac{1}{2}-x\right)\left(j+\frac{1}{2}+x\right)\\ &\quad= \frac{\pi}{\cos\left(\pi x\right)}\prod_{j=0}^{\frac{n}{2}-\frac{1}{2}}\left[\left(j+\frac{1}{2}\right)^2-x^2\right].\end{aligned}$$

References

[1] Paramonov G K and Savva V A 1983 *Phys. Lett.* **97A** 340
[2] Paramonov G K, Savva V A and Samson A M 1985 *Infrared Phys.* **25** 201.
[3] Jakubetz W, Just B, Manz J and Schreier H-J 1990 *J. Phys. Chem.* **94** 2294
[4] Drese K and Holthaus M 1999 *Eur. Phys. J.* D **5** 119
[5] Guerin S and Jauslin H R 2003 *Adv. Chem. Phys.* **125** 1
[6] Yedder A B H, Le Bris C, Atabek O, Chelkowski S and Bandrauk A D 2004 *Phys. Rev.* A **69** 041802(R)
[7] Nest M, Klamroth T and Saalfrank P 2005 *J. Chem. Phys.* **122** 124102
[8] Kanno M, Kato T, Kono H, Fujimura Y and Faisal F H M 2005 *Phys. Rev.* A **72** 033418
[9] Barth I and Manz J 2006 *Angew. Chem. Int. Ed.* **45** 2962
[10] Barth I, Manz J, Shigeta Y and Yagi K 2006 *J. Am. Chem. Soc.* **128** 7043
[11] Barth I and Manz J 2007 *Phys. Rev.* A **75** 012510
[12] Barth I, Manz J and Paramonov G K 2008 *Mol. Phys.* **106** 467
[13] Kamta G L and Bandrauk A D 2005 *Phys. Rev. Lett.* **94** 203003
[14] Krause P, Klamroth T and Saalfrank P 2005 *J. Chem. Phys.* **123** 074105
[15] Palacios A, Bachau H and Martín F 2006 *Phys. Rev. Lett.* **96** 143001
[16] Bandrauk A D, Chelkowski S, Diestler D J, Manz J and Yuan K-J 2008 *Int. J. Mass Spectrom.* **277** 189
[17] Dolya Z E, Nazarova N B, Paramonov G K and Savva V A 1988 *Chem. Phys. Lett.* **145** 499
[18] Barth I, González L, Lasser C, Manz J and Rozgonyi T 2006 *Coherent Control of Molecules* ed B Lasorne and G A Worth (Daresbury: CCP6) p 18
[19] Barth I, Manz J and Sebald P 2008 *Chem. Phys.* **346** 89
[20] Barth I, Manz J, Pérez-Hernández G and Sebald P 2008 *Z. Phys. Chem.* **222** 1311
[21] Barth I, Manz J and Serrano-Andrés L 2008 *Chem. Phys.* **347** 263
[22] Barth I, Serrano-Andrés L and Seideman T 2008 *J. Chem. Phys.* **129** 164303; 2009 *J. Chem. Phys.* **130**, 109901(E)
[23] Došlić N 2006 *Phys. Rev.* A **7**4 013402
[24] Caillat J, Zanghellini J, Kitzler M, Koch O, Kreuzer W and Scrinzi A 2005 *Phys. Rev.* A **71** 012712
[25] Brown A, Meath W J and Tran P 2000 *Phys. Rev.* A **63** 013403
[26] Brown A, Meath W J and Tran P 2002 *Phys. Rev.* A **65** 063401
[27] Uiberacker C and Jakubetz W 2004 *J. Chem. Phys.* **120** 11532
[28] Kitzler M and Lezius M 2005 *Phys. Rev. Lett.* **95** 253001
[29] Chelkowski S and Bandrauk A D 2005 *Phys. Rev.* A **71** 053815
[30] Machholm M and Henriksen N E 2001 *Phys. Rev. Lett.* **87** 193001
[31] Stapelfeldt H and Seideman T 2003 *Rev. Mod. Phys.* **75** 543
[32] Rauch J and Mourou G 2005 *Proc. Am. Math. Soc.* **134** 851
[33] Titchmarsh E C 1948 *Introduction to the Theory of Fourier Integrals* 2nd ed (Oxford University Press) chap VII.7.6
[34] Langhoff S R, Bauschlicher Jr C W and Taylor P R 1988 *J. Chem. Phys.* **88** 5715
[35] Huber K P and Herzberg G 1979 *Molecular Spectra and Molecular Structure* (New York: Van Nostrand Reinhold)
[36] Holthaus M and Just B 1994 *Phys. Rev.* A **49** 1950
[37] Gentle J 2002 *Elements of Computational Statistics* (Springer Science) chap 9.3
[38] Arfken G 1970 *Mathematical Methods for Physicists* 2nd ed (Academic Press) chap 5.10
[39] Whittaker E and Watson G 1958 *A Course of Modern Analysis* 4th ed (Cambridge University Press) chap 2 & 12
[40] Meintrup D and Schäffler S 2005 *Stochastik* (Springer-Verlag) chap 7.4
[41] Ramanujan S 1920 *Q. J. Math.* **48** 294

Tables and table captions

Table 1. Numerical coefficients $c_n = \kappa_n \tau$ of the trigonometric envelope and $c = \kappa\tau$ of the Gaussian envelope for determining the spectral widths $\Gamma_n = c_n \hbar/\tau$ and $\Gamma = c\hbar/\tau$ where κ_n and κ are the full widths at half maximum of $\hat{s}_n^2(k)$ and $\hat{s}^2(k)$, respectively.

n	c_n	n	c_n
1	3.73524	12	2.86200
2	3.29524	13	2.85509
3	3.12772	14	2.84918
4	3.04054	15	2.84405
5	2.98738	16	2.83957
6	2.95169	17	2.83561
7	2.92611	18	2.83210
8	2.90689	19	2.82896
9	2.89193	20	2.82613
10	2.87995	...	...
11	2.87016	∞	2.77259

Table 2. Optimized laser parameters, i.e. laser amplitude $\mathcal{E}_0$ and laser frequency ω, for maximal population transfer in AlCl from $|\Psi_1\rangle = |X\,{}^1\Sigma^+\rangle$ to $|\Psi_2\rangle = |A\,{}^1\Pi_x\rangle$, depending on the effective pulse duration τ and the exponent of the trigonometric envelope n. Both states are separated by an excitation energy of $\hbar\hat{\omega} = 4.79\,\text{eV}$. The phase is always fixed as $\eta = \pi/2$.

	$n = 2$		$n = 5$		$n = 20$		$n = 1000$	
τ (fs)	$\mathcal{E}_0$ (GVm^{-1})	$\hbar\omega$ (eV)	$\mathcal{E}_0$ (GVm^{-1})	$\hbar\omega$ (eV)	$\mathcal{E}_0$ (GVm^{-1})	$\hbar\omega$ (eV)	$\mathcal{E}_0$ (GVm^{-1})	$\hbar\omega$ (eV)
2.5	8.512	4.7495	8.075	4.7558	7.852	4.7589	7.779	4.7598
5.0	4.273	4.7799	4.051	4.7815	3.937	4.7822	3.901	4.7825

Figure captions

Figure 1. Top: Gaussian envelope $s(t)$ (solid) and trigonometric envelopes $s_n(t)$ for $n = 2, 5, 20$ (dotted, dashed, dashed-dotted). Bottom: Squares of the Gaussian envelope $s^2(t)$ (solid) and trigonometric envelopes $s_n^2(t)$ for $n = 2, 5, 20$ (dotted, dashed, dashed-dotted). All four functions have the same full width at half maximum $\tau = 5.0\,\mathrm{fs}$.

Figure 2. Top: Maximal deviation between Gaussian envelope $s(t)$ and trigonometric envelope $s_n(t)$ depending on $\log_{10} n$. For $n = 20$, the maximal deviation is 0.0077. Bottom: Total pulse duration T_n subject to $\log_{10} n$ for $\tau = 2.5\,\mathrm{fs}$ (solid) and $\tau = 5.0\,\mathrm{fs}$ (dashed). The vibrational period of AlCl $T_{vib} = 69\,\mathrm{fs}$ is larger than $T_{20} = 21\,\mathrm{fs}$ and $T_{20} = 42\,\mathrm{fs}$ for $\tau = 2.5\,\mathrm{fs}$ and $\tau = 5.0\,\mathrm{fs}$, respectively.

Figure 3. Time-dependent populations $P_A(t) = |C_2(t)|^2$ of the first excited state $|A\,{}^1\Pi_x\rangle$ for $\tau = 2.5\,\mathrm{fs}$ (top) and $\tau = 5.0\,\mathrm{fs}$ (bottom) and for various exponent values $n = 2, 5, 20, 1000$ (dotted, dashed, dashed-dotted, solid). On the left hand side, the chosen laser parameters maximize the population transfer from $|X\,{}^1\Sigma^+\rangle$ to $|A\,{}^1\Pi_x\rangle$ for the trigonometric pulse with $n = 1000$. On the right hand side, the parameters are optimized for each exponent value $n = 2, 5, 20, 1000$.

Figure 4. Final populations $P_A(T_n/2) = |C_2(T_n/2)|^2$ of the first excited state $|A\,{}^1\Pi_x\rangle$ for $\tau = 2.5\,\mathrm{fs}$ and $\tau = 5.0\,\mathrm{fs}$ versus $\log_{10} n$. The results agree within graphical resolution. The laser parameters are those which optimize the population transfer for $n = 1000$. For $n = 20$, the final population is 0.9998.

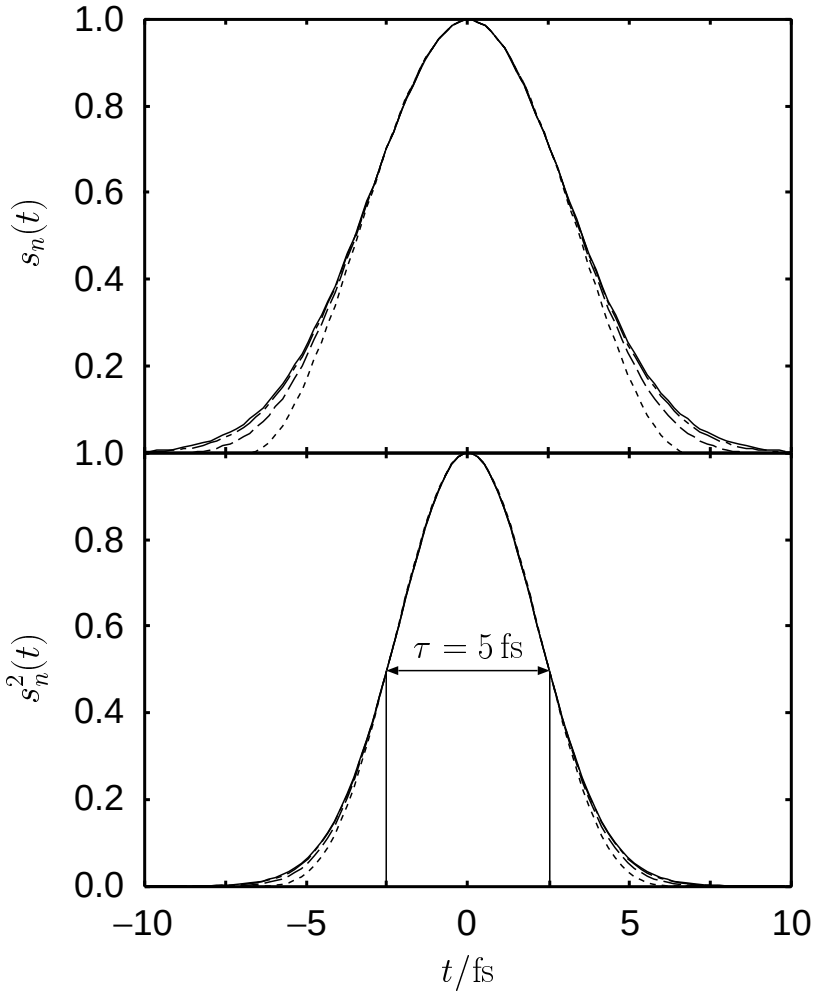
1.0
0.8
0.6
0.4
0.2
1.0
0.8
0.6
0.4
0.2
0.0
$s_n(t)$
$s_n^2(t)$
$\tau = 5\,\mathrm{fs}$
–10
–5
0
5
10
t/fs

Figure 1.

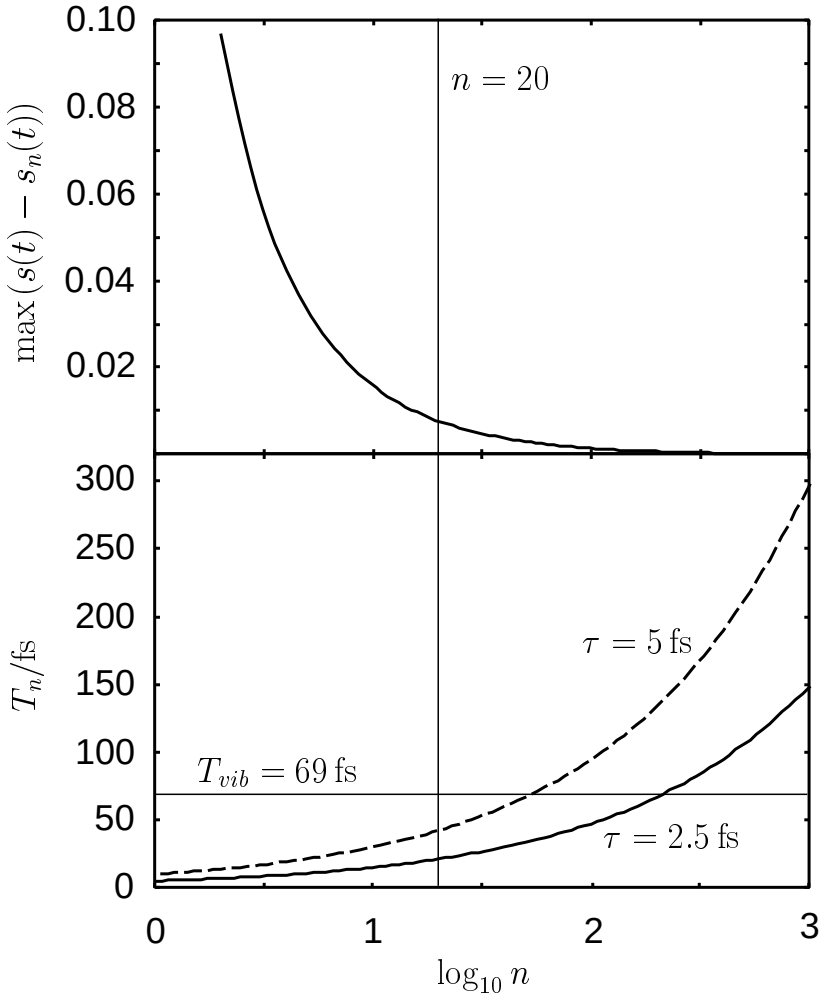
0.10
0.08
0.06
0.04
0.02
$\max(s(t) - s_n(t))$
$n = 20$
300
250
200
150
100
50
0
T_n/fs
$\tau = 5\,\mathrm{fs}$
$T_{vib} = 69\,\mathrm{fs}$
$\tau = 2.5\,\mathrm{fs}$
0
1
2
3
$\log_{10} n$

Figure 2.

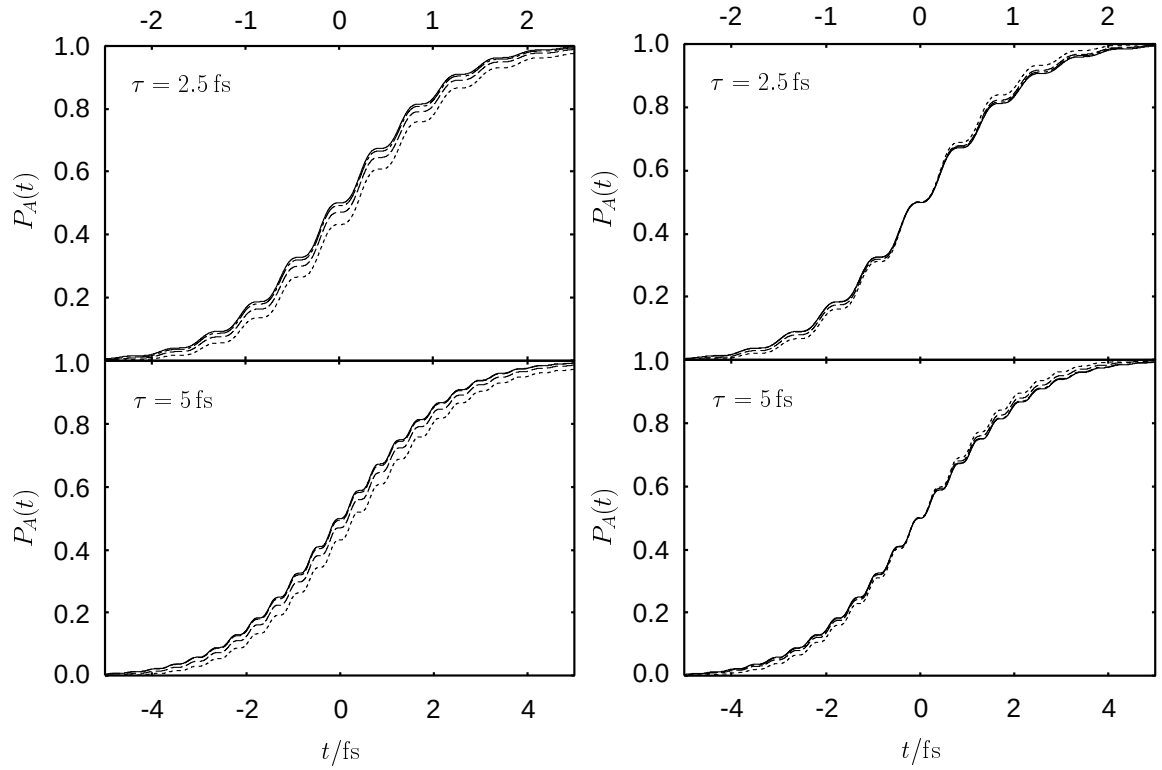

(a) Optimal laser parameters for $n = 1000$.

(b) Optimal laser parameters for each n.

Figure 3.

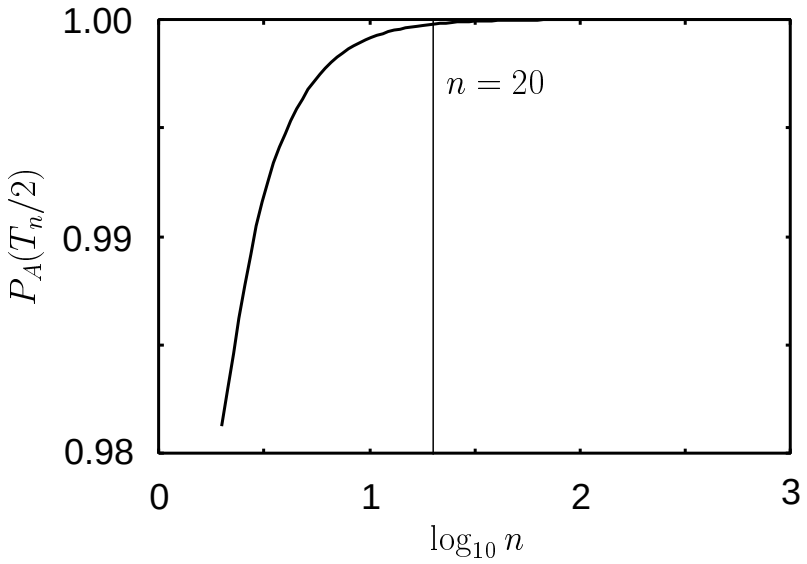

Figure 4.